

Predictive Kinematic Coordinate Control for Aerial Manipulators based on Modified Kinematics Learning

Zhengzhen Li^{1,2}, Jiahao Shen², Mengyu Ji², Huazi Cao^{2,3}, Shiyu Zhao²

Abstract—High-precision manipulation has always been a developmental goal for aerial manipulators. This paper investigates the kinematic coordinate control issue in aerial manipulators. We propose a predictive kinematic coordinate control method, which includes a learning-based modified kinematic model and a model predictive control (MPC) scheme based on weight allocation. Compared to existing methods, our proposed approach offers several attractive features. First, the kinematic model incorporates closed-loop dynamics characteristics and online residual learning. Compared to methods that do not consider closed-loop dynamics and residuals, our proposed method has improved accuracy by 59.6%. Second, a MPC scheme that considers weight allocation has been proposed, which can coordinate the motion strategies of quadcopters and manipulators. Compared to methods that do not consider weight allocation, the proposed method can meet the requirements of more tasks. The proposed approach is verified through complex trajectory tracking and moving target tracking experiments. The results validate the effectiveness of the proposed method.

I. INTRODUCTION

Aerial manipulators have received considerable attention in recent years [1], [2]. An increasing number of research efforts are employing aerial manipulators for tasks unachievable by quadcopters alone. This is primarily due to their ability to combine the rapid mobility of quadcopters with the high-precision manipulation capabilities of manipulators. Compared to quadcopters, aerial manipulators can interact with the environment to accomplish a variety of tasks, such as pick-and-place [3], [4], 3D construction [5], and opening/closing doors [6]. Relative to ground-based manipulators, aerial manipulators can access areas that are challenging for humans or ground robots to reach, significantly expanding the scope of manipulation tasks.

Achieving high-precision control has always been a goal in the research of aerial manipulators. Existing studies achieve high-precision control primarily through two aspects: dynamic control and kinematic control. Dynamic control refers to designing control laws for the quadcopter and the manipulator based on the dynamic model of the aerial manipulator, thereby offsetting the effects of dynamic coupling on the aerial manipulator. Dynamic control methods can be

categorized into two types: the first is decoupled control [7]–[10], where controllers are designed separately for the quadcopter and the manipulator. The second type is coupled control, where a nonlinear model of the entire aerial manipulation system is established to achieve coordinated control [11], [12]. However, starting from dynamic control, only centimeter-level control precision can be obtained because obtaining an accurate dynamic model of aerial manipulator is challenging. To achieve higher precision, research on kinematic control is also essential.

Kinematic control starts from the kinematics of aerial manipulators, focusing on achieving high-precision end-effector control through coordinating the movements of the quadcopter and the manipulator. Kinematic control primarily involves managing the position, velocity, or acceleration within the control state space to achieve precise trajectory tracking of the end-effector. Research in kinematic control primarily addresses two main aspects of these issues.

The first issue is how to achieve high-precision control. Current kinematic control strategies mainly fall into two categories: The first type is closed loop inverse kinematics control (CLIK), which adjusts the kinematic control strategy based on real-time end-effector error, thus achieving high-precision kinematic control [11], [13]. The second method is optimization control, which enhances precision by selecting the optimal control strategy [14]. Compared to CLIK, it ensures strict adherence to physical constraints. An accurate model is a prerequisite for high-precision kinematic planning. However, due to factors such as coupling disturbances between the manipulator and the quadcopter, obtaining an accurate kinematic model of the aerial manipulator is quite challenging.

The second issue is how to allocate and switch control modes. Since the aerial manipulator consists of a quadcopter and a manipulator, its operational modes can be divided into flight mode, coordinated manipulation mode, hover manipulation mode, and configuration adjustment mode. Different modes are adapted to different tasks, making it crucial to select the appropriate mode for specific tasks. Motion allocation can be achieved by adjusting the weights in the kinematic Jacobian matrix [15]. However, it cannot account for physical constraints, which can easily lead to system instability and safety issues. Another common method is optimization control, which ensures high manipulability of the manipulator while minimizing the coupling disturbances it imparts to the quadcopter [16], [17], all under the premise of fulfilling the task. However, fixed weights may not adequately adapt to changes in the environment or to the

This work was supported by National Major Research & Development Plan - Intelligent Robotics Major Special Project (2023YFB4705500) and the Research Center for Industries of the Future at Westlake University (WU2022C027)

Corresponding author: Huazi Cao

¹College of Computer Science and Technology, Zhejiang University, Hangzhou, China. ²WINDY Lab, Department of Artificial Intelligence, Westlake University, Hangzhou, China. ³Westlake Institute for Optoelectronics, Hangzhou, China. {lizhengzhen, shenjiahao, jimengyu, caohuazi, zhaoshiyu}@westlake.edu.cn

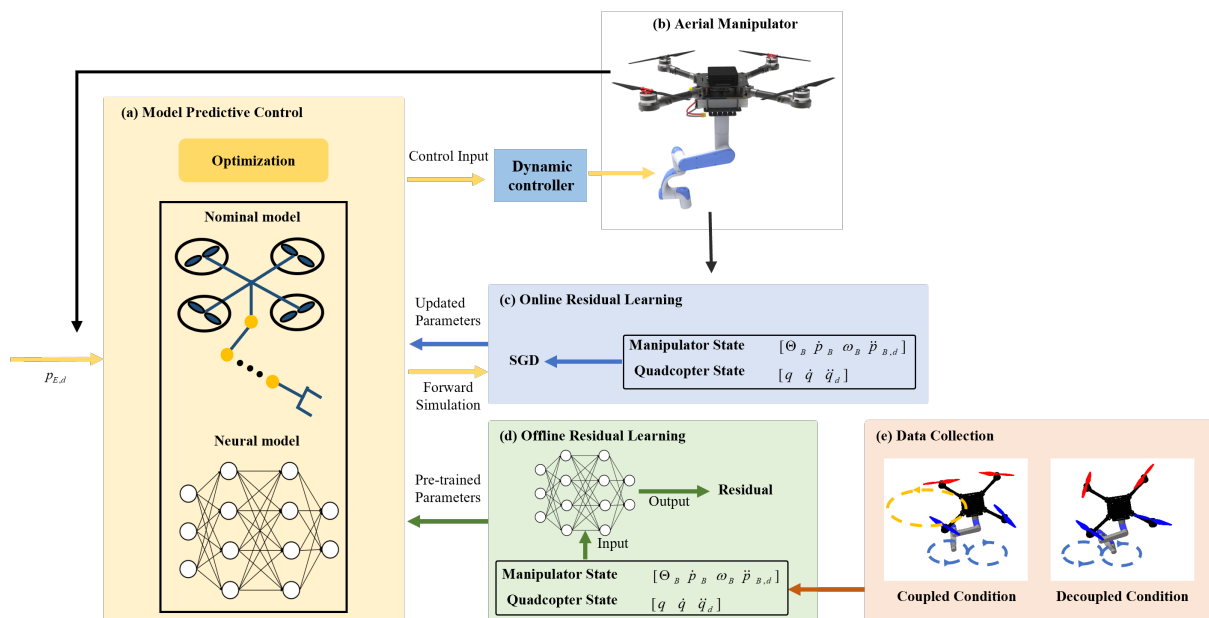


Fig. 1. Schematic of the MPC with learning based modified kinematic model.

requirements of different tasks.

In response to the existing issues of insufficient precision and difficulties in motion allocation, we propose the predictive kinematic coordinate control method. The output of the kinematic controller, after undergoing double integration, serves as the input to the lower level decoupled dynamic controller. The quadcopter employs an extended state observer (ESO) based robust controller in our previous work [7], while the manipulator utilizes a PID controller. Our predictive kinematic coordinate control method is comprised of a learning-based modified kinematic model and a model predictive control (MPC) scheme based on weight allocation, which enables high-precision end-effector kinematic control and coordinated motion allocation. The main novelties of our approach are as follows:

1) We propose a learning-based modified kinematic model for aerial manipulator high precision kinematic control. In the modified kinematic model, the system's dynamic characteristics are considered through an equivalent model, enhancing the precision of kinematic control. Compared to using traditional integral kinematic controller, the average error with the modified kinematic model controller has been reduced by 59.6 %.

2) An MPC approach based on weight allocation has been proposed. Given that the manipulator plays a dominant role during the operational process of the aerial manipulator, we evaluate the mobility of the manipulator and adjust the weights in the MPC objective function to coordinate the motion strategies of both the quadcopter and the manipulator, achieving coordinated control. Compared to methods that do not consider weight allocation, our proposed approach can adapt to a wider range of scenarios and tasks, thereby enhancing the applicability of aerial manipulators.

II. LEARNING-BASED MODIFIED KINEMATIC MODEL

This section describes the learning-based modified kinematic model used for coordinated kinematic control. Our modified kinematic model consists of two parts: the equivalent kinematic model of the quadcopter and the kinematic model of the manipulator.

A. Kinematics of Aerial Manipulator

Let $\mathbf{R}_B \in SO(3)$ denote the rotation matrix of the quadcopter, while $\Theta_B = [\phi_B, \theta_B, \psi_B] \in \mathbb{R}^3$ represents the attitude angle vector of the quadcopter. The quadcopter's position and the end-effector position are denoted by $\mathbf{p}_B, \mathbf{p}_E \in \mathbb{R}^3$, respectively. Let n denote the number of joints in the manipulator, $\mathbf{q} = [q_1, q_2, \dots, q_n]^T \in \mathbb{R}^n$ denote the joint angle vector of the manipulator, and $n = 6$ in this work. The end-effector position in Σ_B is denoted by $\mathbf{p}_E^B \in \mathbb{R}^3$, which can be obtained through the forward kinematics of the manipulator. The relationship between \mathbf{p}_E and \mathbf{p}_E^B is

$$\mathbf{p}_E = \mathbf{p}_B + \mathbf{R}_B \mathbf{p}_E^B. \quad (1)$$

The state space variable is $\xi = [\mathbf{p}_B, \Theta_B, \mathbf{q}] \in \mathbb{R}^{6+n}$. It can be divided into actuated state variables $\xi_c = [\mathbf{p}_B, \psi_B, \mathbf{q}] \in \mathbb{R}^{4+n}$ and underactuated state variables $\xi_u = [\phi_B, \theta_B] \in \mathbb{R}^2$. Differentiating (1) yields [18]:

$$\dot{\mathbf{p}}_E = \mathbf{J}\dot{\xi} = \mathbf{J}_c \dot{\xi}_c + \mathbf{J}_u \dot{\xi}_u, \quad (2)$$

where \mathbf{J}_c and \mathbf{J}_u are actuated Jacobian matrix and underactuated Jacobian matrix, respectively. We leave the details of the \mathbf{J}_c and \mathbf{J}_u for brevity.

B. The Modified Kinematic Model

Ignoring dynamics of the aerial manipulator may result in a reduction in accuracy. To enhance the precision of

kinematic coordinate control, a modified kinematic model including the closed-loop dynamics of the aerial manipulator has been proposed. It incorporates two additional sub-models.

The first sub-model is an modified kinematic model for the quadcopter, established using an equivalent model. The equivalent model can effectively replicate the dynamics of complex systems using a low-order model [19]. The closed-loop dynamics of the quadcopter are related to its flight controller. According to reference [7], the equivalent model of the quadcopter can be simplified as

$$\dot{\mathbf{p}}_B = \mathbf{K}_B(\mathbf{p}_{B,d} - \mathbf{p}_B) + \mathbf{\Delta}, \quad (3)$$

where $\mathbf{p}_{B,d} \in \mathbb{R}^3$ represents the desired position of the quadcopter, $\mathbf{K}_B = \text{diag}([k_{Bx}, k_{By}, k_{Bz}]) \in \mathbb{R}^{3 \times 3}$ represents the constant parameters of the equivalent model, and $\mathbf{\Delta} = [\Delta_x, \Delta_y, \Delta_z]^\top \in \mathbb{R}^3$ denotes the linear residual velocity due to modeling errors and uncertainty disturbances. The modified kinematic model of the quadcopter in aerial manipulator is

$$\begin{aligned} \dot{\mathbf{p}}_{B,d} &= \mathbf{v}_{B,d}, \dot{\mathbf{v}}_{B,d} = \mathbf{a}_{B,d}, \\ \dot{\mathbf{p}}_B &= \mathbf{K}_B(\mathbf{p}_{B,d} - \mathbf{p}_B) + \mathbf{\Delta}. \end{aligned} \quad (4)$$

The second sub-model is the kinematic model of the manipulator. The manipulator exhibits high-speed motion and rapid response, its actual values can be considered equivalent to the desired values. The kinematic model of the manipulator is $\dot{\mathbf{q}} = \mathbf{v}_{q,d}, \dot{\mathbf{v}}_{q,d} = \mathbf{a}_{q,d}$.

Based on the two sub-models, the state space variable of the modified kinematic model can be defined as $\mathbf{x} = [p_{Bx}, \dot{p}_{Bx}, p_{Bx,d}, \dot{p}_{Bx,d}, p_{By}, \dots, q_n, \dot{q}_n]^\top \in \mathbb{R}^{24}$. The residual state variable is defined as $\mathbf{x}_{res} = [0, \Delta_x, 0_{1 \times 3}, \Delta_y, 0_{1 \times 3}, \Delta_z, 0_{1 \times 14}]^\top \in \mathbb{R}^{24}$. Our control input is $\mathbf{u} = [\ddot{p}_{Bx,d}, \ddot{p}_{By,d}, \ddot{p}_{Bz,d}, \ddot{q}_{1,d}, \dots, \ddot{q}_{n,d}]^\top \in \mathbb{R}^9$, which includes the linear accelerations of the quadcopter and the joint accelerations of the manipulator. The control input \mathbf{u} , after undergoing double integration, serves as the input to the lower level decoupled dynamic controller. The quadcopter utilizes an ESO-based robust controller, while the manipulator employs a PID controller. Our state-space model is

$$\mathbf{x}_{k+1} = \mathbf{A}\mathbf{x}_k + \mathbf{B}\mathbf{u}_k + \mathbf{C}\mathbf{x}_{res,k}, \quad (5)$$

where $\mathbf{A} = \text{diag}(\mathbf{A}_1, \mathbf{A}_1, \mathbf{A}_1, \mathbf{A}_2, \dots, \mathbf{A}_2) \in \mathbb{R}^{24 \times 24}$, $\mathbf{B} = \text{diag}(\mathbf{B}_1, \mathbf{B}_1, \mathbf{B}_1, \mathbf{B}_2, \dots, \mathbf{B}_2) \in \mathbb{R}^{24 \times 9}$, and $\mathbf{C} = \text{diag}(\mathbf{C}_1, \mathbf{C}_1, \mathbf{C}_1, \mathbf{O}_{12}) \in \mathbb{R}^{24 \times 24}$. $\mathbf{O}_{12} \in \mathbb{R}^{12 \times 12}$ are zero matrices. $\mathbf{B}_1 = [k\delta_t^3/2, k\delta_t^2/2, \delta_t^2/2, \delta_t]^\top \in \mathbb{R}^4$, where δ_t represents the time interval between two consecutive states, δ_t^2 and δ_t^3 represent the square and cube of δ_t , for the three \mathbf{A}_1 and three \mathbf{B}_1 matrices, k takes values k_{Bx} , k_{By} , and k_{Bz} in sequence. $\mathbf{B}_2 = [\delta_t^2/2, \delta_t]^\top \in \mathbb{R}^2$. $\mathbf{A}_2 = \begin{bmatrix} 1 & \delta_t \\ 0 & 1 \end{bmatrix} \in$

$$\mathbb{R}^{2 \times 2}, \mathbf{A}_1 = \begin{bmatrix} 1 - k\delta_t & 0 & k\delta_t & k\delta_t^2 \\ -k & 0 & k & k\delta_t \\ 0 & 0 & 1 & \delta_t \\ 0 & 0 & 0 & 1 \end{bmatrix} \in \mathbb{R}^{4 \times 4} \text{ and } \mathbf{C}_1 =$$

$$\begin{bmatrix} 0 & \delta_t & 0 & 0 \\ 0 & 1 & 0 & 0 \\ 0 & 0 & 0 & 0 \\ 0 & 0 & 0 & 0 \end{bmatrix} \in \mathbb{R}^{4 \times 4}.$$

C. Residual Learning

In this section, we address the learning of residual $\mathbf{\Delta} \in \mathbb{R}^3$ in the modified kinematic model through neural networks. As shown in Fig 1, our overall residual learning framework consists of two parts: offline residual learning and online residual learning.

For offline residual learning, we employ a feedforward neural network with two hidden layers, each with 32 units, and the ELU activation function is used for each hidden layer [20]. The inputs to the neural network include the quadcopter's roll-pitch-yaw Euler angles, linear velocity, angular velocity $\boldsymbol{\omega}_B \in \mathbb{R}^3$ and joint angles, joint velocities of the manipulator, and control inputs. The output of the neural network is $\mathbf{\Delta}$. We collect data from a 15 cm \times 15 cm \times 10 cm learning space around the manipulator's end-effector in its operational configuration (as shown in Fig 1 (b)). During data collection, the end-effector of the manipulator follows a 8-shape trajectory at different speeds in the 3D space. The quadcopter stay its position or traces circular trajectories with a 10 cm radius at different speeds in the 3D space. Each stage lasts 150 seconds to collect sufficient and informative data.

Online residual learning adjusts the parameters of the final layer of the network in real-time. We define the model prediction error based on the deviation between the predicted state and the actual measured state of the modified kinematic model as $\mathcal{L}_k = \|\hat{\mathbf{p}}_{B,k} - \dot{\mathbf{p}}_{B,k}\|^2$, where \mathcal{L}_k is the model prediction error at time step k , $\hat{\mathbf{p}}_{B,k}$ is the predicted velocity of the learning-based modified kinematic mode and $\dot{\mathbf{p}}_{B,k}$ represent the measured linear velocity of the quadcopter at time step k , respectively. We use stochastic gradient descent (SGD) to adjust the weights of the last layer of the neural network, specifically [20]:

$$\theta_k^\ell = \theta_{k-1}^\ell - \eta \frac{1}{B_l} \sum_{i=k-B_l}^k \nabla \mathcal{L}_i, \quad (6)$$

where θ_k^ℓ and θ_{k-1}^ℓ represent the parameters of the last layer of the neural network at time steps k and $k-1$, respectively, η is the learning rate, and B_l is the batch size. By updating the network parameters using multiple sets of data, online residual learning can be made more stable.

III. MODEL PREDICTIVE CONTROL BASED ON WEIGHT ALLOCATION

This section introduces the proposed MPC framework based on weight allocation. By coordinating the distribution of the weight matrices in the MPC optimization, the framework achieves kinematic coordinate control of the aerial manipulator and facilitates the switching between different motion modes.

A. MPC formulation

The MPC framework formulates the kinematic coordinate control problem as a constrained optimization problem, ensuring that the aerial manipulator strictly adheres to physical constraints and maintains safety during operation. Furthermore, by predicting the position of the quadcopter, the manipulator can be pre-planned to compensate for end-effector deviations caused by discrepancies between the actual and desired states of the quadcopter, thereby enhancing the precision of end-effector kinematic control. Our specific MPC formulation is as follows:

$$\begin{aligned} & \min_u \sum_{k=0}^N J(\mathbf{x}_k, \mathbf{u}_k, \mathbf{x}_{res,k}), \\ \text{s.t. } & \mathbf{x}_{k+1} = \mathbf{A}\mathbf{x}_k + \mathbf{B}\mathbf{u}_k + \mathbf{C}\mathbf{x}_{res,k}, \\ & \mathbf{x}_k \in \mathcal{X}, \mathbf{u}_k \in \mathcal{U}, \\ & \mathbf{x}_0 = \mathbf{x}_{init}, \end{aligned} \quad (7)$$

where (5) defines our state-space kinematic model, and \mathbf{x}_{init} represents the initial state. \mathcal{X} and \mathcal{U} are the boundaries of the state and control variables, respectively. N is the prediction horizon of the MPC, and $J(\mathbf{x}_k, \mathbf{u}_k, \mathbf{x}_{res,k})$ is our objective function.

B. Objective Function

To achieve high-precision manipulation of the aerial manipulator's end-effector and kinematic coordinate control, the objective function consists of four parts, expressed as

$$J(\mathbf{x}_k, \mathbf{u}_k, \mathbf{x}_{res,k}) = J_1 + J_2 + J_3 + J_4. \quad (8)$$

The first part aims to minimize the end-effector tracking error. Specifically, $J_1 = \|\mathbf{J}_c \dot{\xi}_c + \mathbf{J}_u \dot{\xi}_u - \dot{\mathbf{p}}_{E,d}\|_{\mathbf{W}_1}^2$, where $\mathbf{W}_1 \in \mathbb{R}^3$ is a diagonal weight matrix. The desired end-effector velocity can be defined as $\dot{\mathbf{p}}_{E,d} = \dot{\mathbf{p}}_{E,c} - \mathbf{K}_e \mathbf{e}_E$ [21], [22], $\mathbf{K}_e \in \mathbb{R}^{3 \times 3}$ is a diagonal constant matrix, $\dot{\mathbf{p}}_{E,c} \in \mathbb{R}^3$ is the velocity of the target trajectory, and $\mathbf{e}_E = \mathbf{p}_E - \mathbf{p}_{E,d}$ is the end-effector position error, with $\mathbf{p}_E \in \mathbb{R}^3$ and $\mathbf{p}_{E,d} \in \mathbb{R}^3$ representing the current position and the desired position from the target trajectory.

The second part aims to minimize the linear velocity of the quadcopter and joint velocity of the manipulator. Specifically, $J_2 = \|\mathbf{v}_s\|_{\mathbf{W}_2}^2$, where $\mathbf{v}_s = [\dot{p}_{Bx}, \dot{p}_{By}, \dot{p}_{Bz}, \dot{q}_1, \dots, \dot{q}_n]^T \in \mathbb{R}^9$ and $\mathbf{W}_2 \in \mathbb{R}^9$ is a diagonal weight matrix. Optimizing \mathbf{v}_s can achieve coordinated motion allocation between the quadcopter and the manipulator.

The third part aims to minimize the control inputs, defined as $J_3 = \|\mathbf{u}\|_{\mathbf{W}_3}^2$, where $\mathbf{W}_3 \in \mathbb{R}^9$ is a diagonal weight matrix. Minimizing the control inputs helps to avoid drastic changes in the control signals, conserving energy and extending the manipulation time of aerial manipulators.

The fourth part ensures that during manipulation, the end-effector remains within the model's learning space. Specifically, $J_4 = \|\mathbf{p}_E^B - \mathbf{p}_O^B\|_{\mathbf{W}_4}^2$, \mathbf{p}_O^B is the position of the center of the learning space in the quadcopter's body frame, and $\mathbf{W}_4 \in \mathbb{R}^3$ is a diagonal weight matrix. It can ensuring high

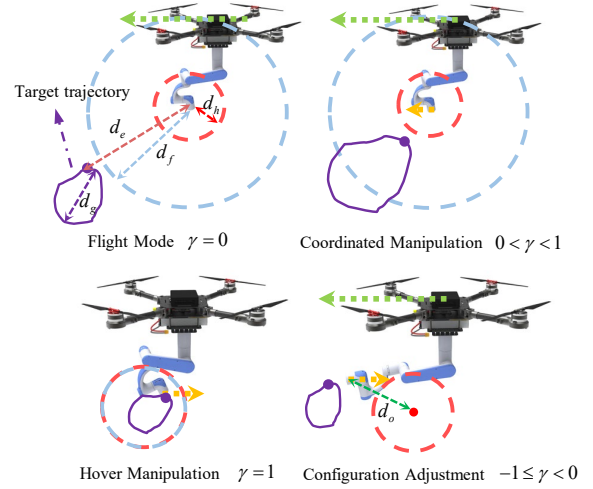


Fig. 2. Different mode of the Aerial Manipulator. The red and blue circles represent State Transition Boundaries.

manipulability and precision while preventing excessive manipulator movements that could cause significant quadcopter instability.

C. Weight Allocation

Our allocation strategy consists of three steps: first, the desired motion state of the manipulator is evaluated; second, the weights are adjusted based on the evaluation; finally, the MPC controls the aerial manipulator according to the adjusted weights. To better evaluate the desired motion state of the manipulator, we define $\gamma \in [-1, 1]$ as a metric for the expected motion, Specifically:

$$\gamma = \begin{cases} 0 & \text{if } d_e > d_f, \\ \frac{k_{mp} + d_h}{k_{mp} + d_e} & \text{if } d_h < d_e \leq d_f \text{ and } d_o < d_h, \\ 1 & \text{if } d_e \leq d_h, d_o < d_h \text{ and } d_g < d_h, \\ -k_{mn} \frac{d_o - d_h}{d_{edge} - d_h} & \text{if } d_o \geq d_h, \end{cases} \quad (9)$$

where d_e is the distance between the end-effector and the target trajectory (as shown in Fig 2.); d_f is the boundary for switching between flight mode and manipulation mode; d_h is the boundary for switching between the hover manipulation mode and other modes and it is related to the boundary of the learning space; d_o represents the distance from the end-effector to the center of the learning space; d_g represents the maximum diameter of the target trajectory; d_{edge} represents the maximum distance from the center of the manipulation space to the edge of the manipulator's workspace; k_{mp} and k_{mn} are constants greater than 0. The value of d_f depends on two cases: when the target trajectory cannot be fully covered by the hover manipulation space, d_f is a large fixed boundary, and the system enters coordinated manipulation mode ($0 < \gamma < 1$) after the flight approaches the target trajectory; when the size of the target trajectory d_g is smaller than the hover manipulation boundary, $d_f = d_h$, it enters the hover manipulation mode ($\gamma = 1$) after the flight mode

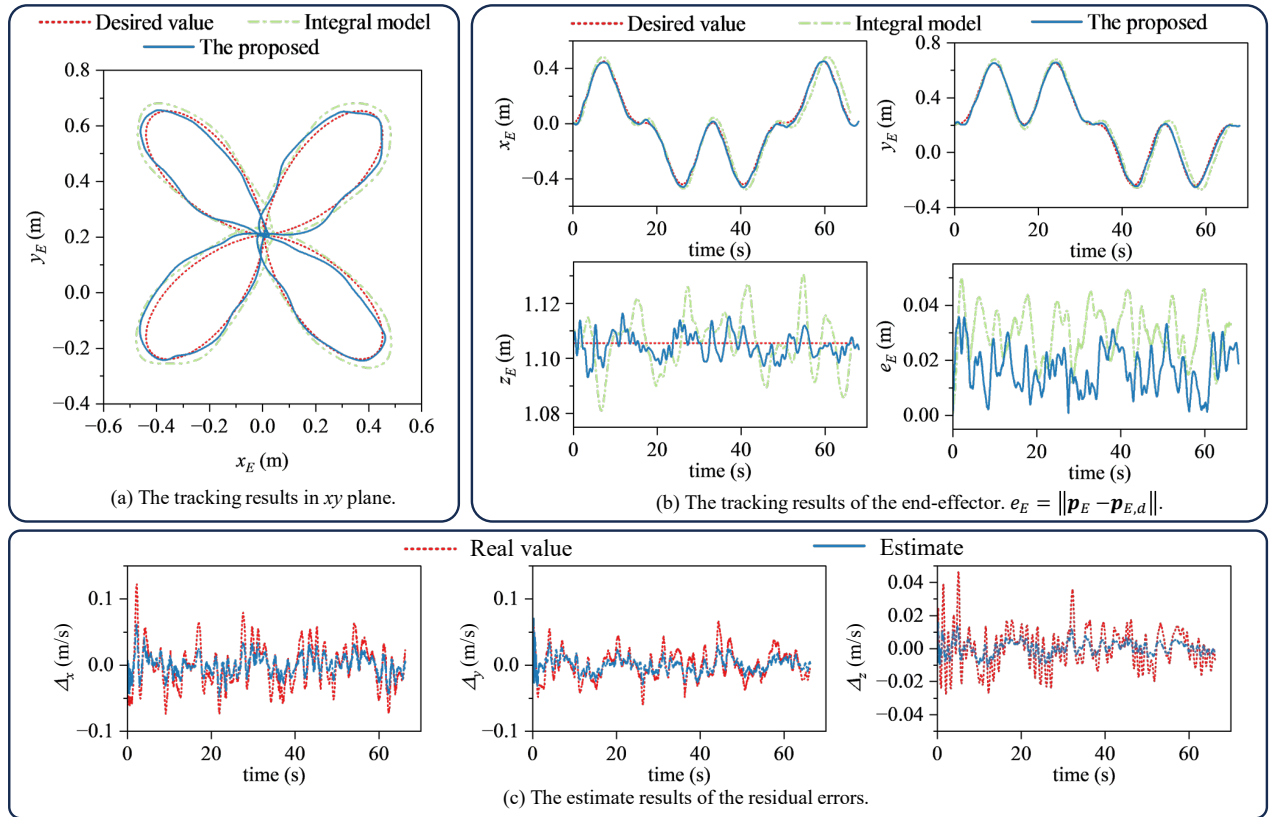


Fig. 3. The results of the complex trajectory tracking experiment.

approaches the target. When d_e is large, the system remains in flight mode, where $\gamma = 0$. d_o is used to assess whether the manipulator end-effector is within the learning space. If it exceeds the workspace, $-1 \leq \gamma < 0$. In configuration adjustment mode, the end-effector of the manipulator moves towards the learning space, while the quadcopter moves towards the target trajectory to ensure the trajectory tracking performance of the aerial manipulator end-effector.

The second part involves adjusting the weight matrices in the MPC objective function. Adjusting \mathbf{W}_2 changes the velocity of the quadcopter and manipulator, while adjusting \mathbf{W}_4 ensures that the manipulator stays close to the learning space. Specifically, $\mathbf{W}_2 = \mathbf{A}_2 \mathbf{W}_{2,0}$ and $\mathbf{W}_4 = w_d \mathbf{W}_{4,0}$, where $\mathbf{W}_{2,0}$ and $\mathbf{W}_{4,0}$ are the initial weight matrices. $\mathbf{A}_2 = \text{diag}([w_q, w_q, w_q, w_m, \dots, w_m]) \in \mathbb{R}^{9 \times 9}$, where w_q and w_m are parameters adjust the velocity of the quadcopter and the manipulator, respectively, and the parameter w_d adjusting the weight in the objective function to bring the manipulator's end-effector closer to the center of the learning space. The specific definitions are

$$w_q = k_q(\gamma^2 + 0.1), w_m = \frac{k_m}{\gamma + 0.01}, w_d = \frac{k_d d_o}{1.1 + \gamma}, \quad (10)$$

where k_q , k_m , and k_d are constants greater than 0. As $|\gamma|$ increases, we decrease w_m and increase w_q , thereby increasing the movement weight of the manipulator in the MPC while reducing the movement weight of the quadcopter.

Algorithm 1: MPC based on weight allocation

```

1 Input:  $d_g, \mathbf{p}_E, \mathbf{p}_{E,d}, \mathbf{x}_k, d_e, d_o, \theta_{k-1}^\ell$ ;
2 Output:  $\mathbf{a}_{B,d}, \ddot{\mathbf{q}}_d$ ;
3 function MPC( $d_g, \mathbf{p}_E, \mathbf{p}_{E,d}, \mathbf{x}_k$ );
4      $\gamma \leftarrow$  calculating (9);
5      $w_q, w_m, w_d \leftarrow$  calculating (10);
6      $\mathbf{J} \leftarrow$  calculating (8);
7     NN residual model update  $\leftarrow$  calculating (6);
8     update modified kinematic model using (4);
9      $\mathbf{a}_{B,d}, \ddot{\mathbf{q}}_d \leftarrow$  calculating (7);
10    return  $\mathbf{a}_{B,d}, \ddot{\mathbf{q}}_d$ ;
11 end function

```

IV. EXPERIMENTAL VALIDATION

In this section, we validate the proposed method by two numerical experiments.

A. Experimental Setup

The quadcopter used in this study has a diagonal wheel-base of 0.93 m, with a length and width of 1.37 m and a height of 0.12 m. Its mass is 2.6 kg. The manipulator is mounted beneath the quadcopter, with a total mass of 1.2 kg. We validated our algorithm in Gazebo. The quadcopter uses a ESO-based robust controller, running in a PX4 environment at a frequency of 100 Hz. The details can be

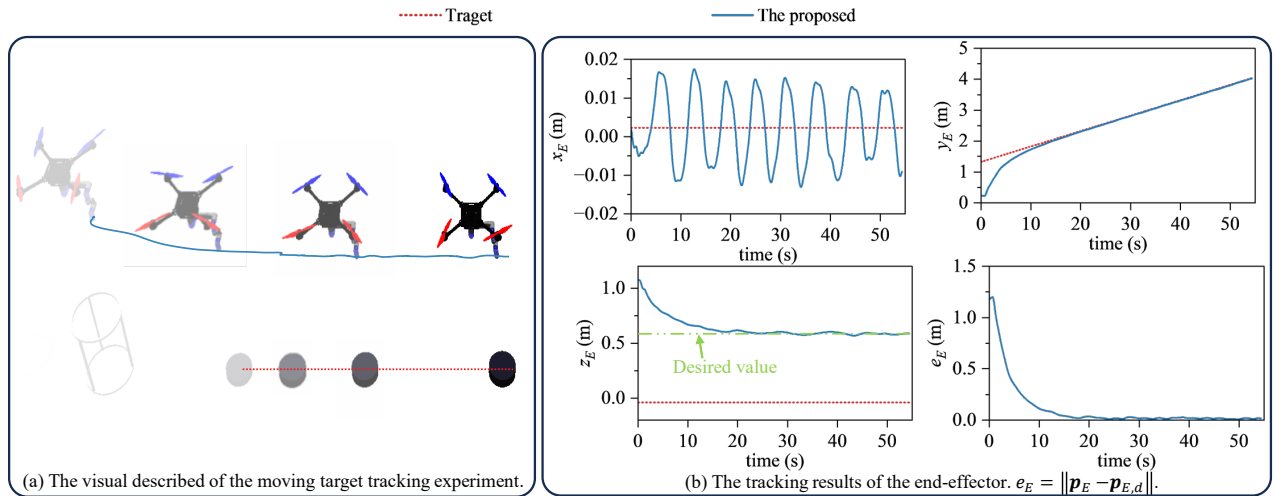


Fig. 4. The results of the moving target tracking experiment.

found in our previous work [7]. The neural network of offline residual learning is implemented in Pytorch, while the online residual learning updates the parameters in C++. The MPC is implemented through the acados [23] framework with a horizon $N = 15$ and planning frequency of 50 Hz. In all simulations, we used the same control gains, with the modified kinematic parameters set to $\mathbf{K}_B = \text{diag}([6.67, 6.67, 2.38])$. The learning rates η were set to 0.01 for offline residual learning and 0.0015 for online residual learning, with a batch size $B_l = 20$. The matrix $\mathbf{K}_e = \text{diag}([0.8, 1.2, 1.2])$, the values of k_q was set to 1000, k_m was set to 10 and k_d was set to 100, the values of k_{mn}, k_{mp} were set to 1. The parameters d_{edge}, d_f, d_h were set to 0.38 m, 1.0 m, and 0.075 m, respectively.

B. Complex Trajectory Tracking Experiment

The purpose of this experiment is to verify that the end-effector can track complex trajectories under the proposed algorithm framework. The desired trajectory is a four-leaf clover pattern. The desired trajectory of the end-effector is given in Fig 3(a).

The tracking performance of the end-effector is shown in Fig 3, and the integral model is a model that does not consider dynamic characteristics. From Fig 3 (b), the average position error of the proposed method is 0.0122 m, compared to 0.0302 m for MPC using the integral model, the proposed method improved accuracy by 59.6%, which demonstrates the effectiveness of our learning-based modified kinematic model. Fig 3 (c) is the estimate results of residual errors, it indicates that our neural network can accurately estimate the trend of changes in uncertainty disturbances.

C. Moving Target Tracking Experiment

The purpose of this experiment is to verify that the aerial manipulator can achieve coordinated motion across different modes under the proposed algorithm framework. The initial coordinates of the aerial manipulator end-effector and the moving target are $[0, 0.2, 1.2]^T$ m and $[0, 1.4, 0]^T$ m,

respectively. The moving target moves along the positive y-axis at a speed of 0.05 m/s. The aerial manipulator is required to start from the hover position, catch up with the moving target, and follow it at a height of 0.6 m above the target.

As shown in Fig 4, the aerial manipulator catches up with the target at around 15 seconds and follows it smoothly. The trajectory throughout the process is relatively smooth, indicating that the aerial manipulator can stably switch from hover mode to flight mode and then to coordinated mode. The manipulator approaches the object within 5 seconds and enters a stable tracking state after 15 seconds. The average error during stable end-effector tracking is 0.0197 m. This demonstrates the high-precision kinematic coordinate control across different modes, verifying the effectiveness of our kinematic coordinate control method.

V. CONCLUSIONS

This paper proposes a predictive kinematic coordinate control method, which includes a learning based modified kinematic model and a MPC scheme based on weight allocation. The method is validated through two experimental results. The first experiment shows that, compared to MPC using the integral model, the proposed method reduces the average error by 59.6%, verifying the effectiveness of our learning-based modified kinematic model for high-precision control. The second experiment demonstrates that our aerial manipulator can quickly approach the target and stably follow its motion, proving the effectiveness of our motion allocation strategy. Although we have achieved improvements in trajectory accuracy and coordinated tracking of moving targets, validating the algorithm on a physical platform rather than in simulation would provide stronger conclusions. Our residual learning model can effectively predict the residuals and ensure that MPC achieves a control frequency of 50 Hz, there is still room for improvement in residual learning. In the future, we aim to enhance the residual learning capability while maintaining the real-time performance of MPC.

REFERENCES

- [1] A. Ollero, M. Tognon, A. Suarez, D. Lee, and A. Franchi, "Past, present, and future of aerial robotic manipulators," *IEEE Transactions on Robotics*, vol. 38, no. 1, pp. 626–645, 2021.
- [2] N. Staub, D. Bicego, Q. Sabl , V. Arellano, S. Mishra, and A. Franchi, "Towards a flying assistant paradigm: The othex," in *2018 IEEE International Conference on Robotics and Automation (ICRA)*, pp. 6997–7002, IEEE, 2018.
- [3] M. Wang, Z. Chen, K. Guo, X. Yu, Y. Zhang, L. Guo, and W. Wang, "Millimeter-level pick and peg-in-hole task achieved by aerial manipulator," *IEEE Transactions on Robotics*, 2023.
- [4] W. Luo, J. Chen, H. Ebel, and P. Eberhard, "Time-optimal handover trajectory planning for aerial manipulators based on discrete mechanics and complementarity constraints," *IEEE Transactions on Robotics*, 2023.
- [5] K. Zhang, P. Chermprayong, F. Xiao, D. Tzoumanikas, B. Dams, S. Kay, B. B. Kocer, A. Burns, L. Orr, T. Alhinai, *et al.*, "Aerial additive manufacturing with multiple autonomous robots," *Nature*, vol. 609, no. 7928, pp. 709–717, 2022.
- [6] M. Orsag, C. Korpela, S. Bogdan, and P. Oh, "Valve turning using a dual-arm aerial manipulator," in *2014 international conference on unmanned aircraft systems (ICUAS)*, pp. 836–841, IEEE, 2014.
- [7] H. Cao, Y. Li, C. Liu, and S. Zhao, "Eso-based robust and high-precision tracking control for aerial manipulation," *IEEE Transactions on Automation Science and Engineering*, vol. 21, no. 2, pp. 2139–2155, 2023.
- [8] Y.-C. Liu and C.-Y. Huang, "Ddpg-based adaptive robust tracking control for aerial manipulators with decoupling approach," *IEEE Transactions on Cybernetics*, vol. 52, no. 8, pp. 8258–8271, 2021.
- [9] D. Lee, H. Seo, I. Jang, S. J. Lee, and H. J. Kim, "Aerial manipulator pushing a movable structure using a dob-based robust controller," *IEEE Robotics and Automation Letters*, vol. 6, no. 2, pp. 723–730, 2020.
- [10] S. Kim, S. Choi, H. Kim, J. Shin, H. Shim, and H. J. Kim, "Robust control of an equipment-added multirotor using disturbance observer," *IEEE Transactions on Control Systems Technology*, vol. 26, no. 4, pp. 1524–1531, 2017.
- [11] H. Yang and D. Lee, "Dynamics and control of quadrotor with robotic manipulator," in *2014 IEEE international conference on robotics and automation (ICRA)*, pp. 5544–5549, IEEE, 2014.
- [12] B. Y ksel, G. Buondonno, and A. Franchi, "Differential flatness and control of protocentric aerial manipulators with any number of arms and mixed rigid-/elastic-joints," in *2016 IEEE/RSJ International Conference on Intelligent Robots and Systems (IROS)*, pp. 561–566, IEEE, 2016.
- [13] E. Cataldi, F. Real, A. Su rez, P. Di Lillo, F. Pierri, G. Antonelli, F. Caccavale, G. Heredia, and A. Ollero, "Set-based inverse kinematics control of an anthropomorphic dual arm aerial manipulator," in *2019 International Conference on robotics and automation (ICRA)*, pp. 2960–2966, IEEE, 2019.
- [14] D. Lunni, A. Santamaria-Navarro, R. Rossi, P. Rocco, L. Bascetta, and J. Andrade-Cetto, "Nonlinear model predictive control for aerial manipulation," in *2017 International Conference on Unmanned Aircraft Systems (ICUAS)*, pp. 87–93, IEEE, 2017.
- [15] H. Xing, A. Torabi, L. Ding, H. Gao, Z. Deng, and M. Tavakoli, "Enhancement of force exertion capability of a mobile manipulator by kinematic reconfiguration," *IEEE Robotics and Automation Letters*, vol. 5, no. 4, pp. 5842–5849, 2020.
- [16] M. Geisert and N. Mansard, "Trajectory generation for quadrotor based systems using numerical optimal control," in *2016 IEEE international conference on robotics and automation (ICRA)*, pp. 2958–2964, IEEE, 2016.
- [17] N. Imanberdiyev and E. Kayacan, "Redundancy resolution based trajectory generation for dual-arm aerial manipulators via online model predictive control," in *IECON 2020 The 46th Annual Conference of the IEEE Industrial Electronics Society*, pp. 674–681, IEEE, 2020.
- [18] R. Chen, Q. Liu, Z. Chen, K. Guo, X. Yu, and L. Guo, "Online trajectory generation for aerial manipulator subject to multi-tasks and inequality constraints," in *2023 International Conference on Unmanned Aircraft Systems (ICUAS)*, pp. 933–939, IEEE, 2023.
- [19] J. Zou, C. Peng, Y. Yan, H. Zheng, and Y. Li, "A survey of dynamic equivalent modeling for wind farm," *Renewable and Sustainable Energy Reviews*, vol. 40, pp. 956–963, 2014.
- [20] A. Saviolo, J. Frey, A. Rathod, M. Diehl, and G. Loianno, "Active learning of discrete-time dynamics for uncertainty-aware model predictive control," *IEEE Transactions on Robotics*, 2023.
- [21] H. Cao and S. Zhao, "Predictive damped inverse kinematics for redundant and underactuated robotic systems," in *2020 IEEE 16th International Conference on Control & Automation (ICCA)*, pp. 348–353, IEEE, 2020.
- [22] M. Faroni, M. Beschi, N. Pedrocchi, and A. Visioli, "Predictive inverse kinematics for redundant manipulators with task scaling and kinematic constraints," *IEEE Transactions on Robotics*, vol. 35, no. 1, pp. 278–285, 2018.
- [23] R. Verschueren, G. Frison, D. Kouzoupis, J. Frey, N. v. Duijkeren, A. Zanelli, B. Novoselnik, T. Albin, R. Quirynen, and M. Diehl, "acados—a modular open-source framework for fast embedded optimal control," *Mathematical Programming Computation*, vol. 14, no. 1, pp. 147–183, 2022.